Received: 14 December 2017 | Accepted: 12 February 2018

DOI: 10.1002/prp2.391

ORIGINAL ARTICLE

Electrical dynamics of isolated cerebral and skeletal muscle endothelial tubes: Differential roles of G-protein-coupled receptors and K^+ channels

Md A. Hakim | John N. Buchholz | Erik J. Behringer

Basic Sciences, Loma Linda University, Loma Linda, CA, USA

Correspondence
Erik J. Behringer, Department of Basic Sciences, Loma Linda University, Loma Linda, CA, USA.
Email: ebehringer@llu.edu

Funding information
National Institutes of Health, Grant/Award Number: 5R00AG047198

Abstract

Electrical dynamics of freshly isolated cerebral endothelium have not been determined independently of perivascular nerves and smooth muscle. We tested the hypothesis that endothelium of cerebral and skeletal muscle arteries differentially utilizes purinergic and muscarinic signaling pathways to activate endothelium-derived hyperpolarization. Changes in membrane potential (V_m) were recorded in intact endothelial tubes freshly isolated from posterior cerebral and superior epigastric arteries of male and female C57BL/6 mice (age: 3-8 months). V_m was measured in response to activation of purinergic (P2Y) and muscarinic (M_3) receptors in addition to small- and intermediate-conductance Ca^{2+}-activated K^+ (SK_{Ca}/IK_{Ca}) and inward rectifying K^+ (K_{IR}) channels using ATP (100 $\mu mol \cdot L^{-1}$), acetylcholine (ACh; 10 $\mu mol \cdot L^{-1}$), NS309 (0.01-10 $\mu mol \cdot L^{-1}$), and 15 $mmol \cdot L^{-1}$ KCl, respectively. Intercellular coupling was demonstrated via transfer of propidium iodide dye and electrical current (±0.5-3 nA) through gap junctions. With similarities observed across gender, peak hyperpolarization to ATP and ACh in skeletal muscle endothelial tubes was ~twofold and ~sevenfold higher, respectively, vs cerebral endothelial tubes, whereas responses to NS309 were similar (from resting V_m ~−30 mV to maximum ~−80 mV). Hyperpolarization (~8 mV) occurred during 15 $mmol \cdot L^{-1}$ KCl treatment in cerebral but not skeletal muscle endothelial tubes. Despite weaker hyperpolarization during endothelial GPCR stimulation in cerebral vs skeletal muscle endothelium, the capability for robust SK_{Ca}/IK_{Ca} activity is preserved across brain and skeletal muscle. As vascular reactivity decreases with aging and cardiovascular disease, endothelial K^+ channel activity may be calibrated to restore blood flow to respective organs regardless of gender.

KEYWORDS
calcium-activated K^+ channels, endothelium-derived hyperpolarization, muscarinic, purinergic

Abbreviations: $[Ca^{2+}]_i$, intracellular Ca^{2+} concentration; $[Ca^{2+}]_o$, extracellular Ca^{2+} concentration; $[K^+]_o$, extracellular K^+ concentration; ACh, acetylcholine; ATP, adenosine triphosphate; EDH, endothelium-derived hyperpolarization; E_K, equilibrium potential for K^+; GPCR, G-protein-coupled receptor; K_{IR} channel, inward-rectifying K^+ channel; M_3, muscarinic receptor type 3; NO, nitric oxide; P2Y, purinergic receptor type 2Y; PCA, posterior cerebral artery; pEC_{50}, negative log of the half-maximal concentration; PSS, physiological salt solution; SEA, superior epigastric artery; SK_{Ca}/IK_{Ca} channels, small- and intermediate-conductance Ca^{2+}-activated K^+ channels; V_m, membrane potential.

1 | INTRODUCTION

Endothelium-derived hyperpolarization (EDH) entails activation of small- and intermediate- conductance Ca^{2+}-activated K^+ (SK_{Ca}/IK_{Ca}) channels and increased plasma membrane potential (V_m).[1,2] With the exception of capillaries,[3] SK_{Ca}/IK_{Ca} channels play a substantial role in vascular resistance networks throughout the body and are thereby integral to tissue blood flow and oxygen delivery.[4] As a "nonexcitable" tissue, the endothelium depends on elevated intracellular Ca^{2+} ($[Ca^{2+}]_i$) to activate voltage-insensitive SK_{Ca}/IK_{Ca} channels to hyperpolarize cells while enhancing the electrochemical gradient by which extracellular Ca^{2+} ions enter the cell interior.[5,6] A parallel vasodilator pathway entails the production of nitric oxide (NO), also sensitive to increases in $[Ca^{2+}]_i$.[7,8] Thus, via hyperpolarization-induced Ca^{2+} entry, SK_{Ca}/IK_{Ca} channels have also been implicated in the enhanced production of NO[9] while effectively serving as a feed-forward mechanism of the EDH pathway.[5,10] Thus, the SK_{Ca}/IK_{Ca} channels have altogether emerged as important therapeutic targets for cardiovascular disease.[11]

In order to understand native endothelial function independent of the added complexity of perivascular nerve and smooth muscle function, fresh skeletal muscle arterial endothelial tubes have been examined extensively for their fundamental Ca^{2+} and electrical signaling dynamics.[12,13] Despite our current understanding of EDH in peripheral skeletal muscle, whereby a dynamic increase (10- to 100-fold) in blood flow can take place from inactivity to maximal aerobic exercise,[14,15] this identical examination of cerebral arterial endothelium underlying central blood flow distribution to the brain has not been examined. In the long-term, such investigation may provide new insight into healthy brain maturation during aging[16] as well as the pathogenesis of chronic diseases (eg, hemorrhagic stroke, dementia).[17,18]

The goal of this study was to conduct a comparative analysis of electrical dynamics across cerebral and skeletal muscle endothelium in response to activation of classical G-protein-coupled receptors [GPCRs; purinergic type 2Y (P2Y), muscarinic type 3 (M_3) receptors] and K^+ channels [SK_{Ca}/IK_{Ca}, inward rectifying K^+ (K_{IR}) channels]. In turn, we addressed whether gender itself has an effect on the pharmacological regulation of endothelial V_m. We tested the central hypothesis that endothelial tubes isolated from cerebral and skeletal muscle arteries differentially utilize purinergic and muscarinic signaling pathways to activate EDH. Intact endothelium was freshly isolated from the posterior cerebral arteries (PCAs) and superior epigastric arteries (SEAs) of young adult C57BL/6 mice (age: 3-8 months). Changes in V_m were measured in response to adenosine triphosphate (ATP), acetylcholine (ACh), NS309, elevated extracellular K^+ ($[K^+]_o$), and current injection (hyperpolarizing and depolarizing). In brief, skeletal muscle and cerebral endothelial tubes responded differently to classical endothelial GPCR agonists and K_{IR} channel activation but SK_{Ca}/IK_{Ca} channel function was preserved. In addition, there were no significant differences observed across genders in these young animals during respective treatment conditions.

2 | MATERIALS AND METHODS

2.1 | Animal care and use

All animal care use and experimental protocols were approved by the Institutional Animal Care and Use Committee (IACUC; Protocol #8150028) of Loma Linda University and performed in accord with the National Research Council's "*Guide for the Care and Use of Laboratory Animals*" (8th Edition, 2011) and the ARRIVE guidelines.[19,20] Mice were housed on a 12:12 hour light-dark cycle at 22°C-24°C with fresh water and food available ad libitum. Animal housing was overseen by the Animal Care Facility at Loma Linda University. Mice were housed as 2-5 animals of the same gender per cage with enriched environments (eg, toys in cages) and checked daily for fresh water and food, activity level, and physical appearance by experienced animal technicians. Routine visits were also performed by campus veterinarians available at all times.

Experiments were performed on C57BL/6 young mice (3-8 months old; male & female, n = 16 each) obtained from the National Institute on Aging colonies at Charles River Laboratories (Wilmington, MA, USA). All animals were allowed to acclimate to their housing environment for at least 1 week before experimentation and one mouse was studied per day. Animals were selected randomly with respect to gender and the arterial endothelium type (cerebral or skeletal muscle) examined.

2.2 | Solutions

Physiological salt solution [(PSS); composition in $mmol \cdot L^{-1}$: 140 NaCl, 5 KCl, 2 $CaCl_2$, 1 $MgCl_2$, 10 HEPES, 10 glucose; pH 7.4, 295-300 mOsm] maintained the health of freshly isolated and intact endothelial tubes during all experiments. During blood vessel isolation, the PSS dissection buffer lacked $CaCl_2$ and contained filtered 0.1% BSA (Bovine Serum Albumin, A7906, Sigma). For dissociation of endothelium from smooth muscle, the PSS dissociation buffer contained a reduced Ca^{2+} concentration (0.1 $mmol \cdot L^{-1}$ $CaCl_2$), 0.1% BSA, and an enzyme cocktail (see below in *Endothelial tube isolation and superfusion*). For solutions with nominally zero extracellular Ca^{2+} concentration ($[Ca^{2+}]_o$) or 15 $mmol \cdot L^{-1}$ KCl, equimolar increases or decreases of NaCl maintained osmolarity. Reagents were purchased from Sigma-Aldrich (St. Louis, MO, USA) or ThermoFisher Scientific (Pittsburgh, PA, USA) unless otherwise indicated; corresponding catalog numbers are shown in parentheses for nonstandard reagents or chemicals.

2.3 | Surgery and microdissection

Each animal was anesthetized via inhalation of isoflurane followed by decapitation. The PCA and SEA were chosen as representative vascular endothelial study models for the brain and skeletal muscle, respectively. The electrical dynamics and structural integrity of respective isolated and intact endothelial tubes (width: ≥50 μm, length: ≥300 μm) facilitated measurements of intra- and intercellular

signaling along and among endothelial cells. In addition, studies of the rodent PCA[21-23] and SEA[12] are substantially represented in the literature and altogether encompass examination of fundamental endothelial signaling mechanisms, vascular development/aging, and pathology.

All dissection procedures required specimen magnification via stereomicroscopes (Stemi 2000 & 2000-C, Zeiss, NY, USA) and illumination provided by fiber optic light sources (Fostec 8375, Schott, Mainz, Germany & KL200, Zeiss). Macrodissection procedures included removal of the brain and abdominal skeletal muscles for cerebral arteries and skeletal muscle arteries, respectively, using sharp dissection scissors [RS-5912, Roboz Surgical Instruments, Gaithersburg, MD, USA; 14393 & 15905, World Precision Instruments (or WPI), Sarasota, FL, USA] and forceps [coarse-tipped straight (RS-4960; Dumostar) & bone-cutting (RS-8480; Roboz)]. For microdissection to remove respective arteries, the brain or abdominal muscles were placed in chilled (4°C) PSS dissection buffer and secured using stainless steel pins (Living Systems Instrumentation, St. Albans City, VT, USA) in a glass petri dish (diameter: 9 cm, depth: 2.25 cm) containing a charcoal Sylgard coated bottom (depth: 0.75 cm) (Dow-Corning, Auburn, MI, USA). Microdissection instruments included Vannas style scissors [555640S (9.5 mm blades) & 14364 (3 mm blades), WPI; Moria MC52 (7 mm blades) & 15000-00 (3 mm blades), Fine Science Tools (or FST), Foster City, CA, USA] and sharpened fine-tipped forceps (Dumont #5 & Dumont #55, FST). A customized stainless steel chamber apparatus containing a circular receptacle (diameter: 9.5 cm, depth: 2.5 cm) and surrounding cooling reservoir [diameter: 12.5 cm, depth: 9 cm; filled with a 1:1 coolant mixture of water and laboratory grade ethylene glycol as continuously cycled using a recirculating chiller (Isotemp 500LCU, ThermoFisher)] was used to maintain temperature of PSS in the dissection petri dish.

2.3.1 | Cerebral arteries

While viewing through a stereomicroscope, an incision was made using only the tips of dissection scissors starting with the occipital bone and extending up through the nasal bone of the skull. The skull was carefully opened along the incision, whereas connective tissue was separated from the brain with an intact circle of Willis. The brain was then secured ventral side facing up in the chamber containing chilled dissection PSS. Posterior cerebral arteries (0.5-1 cm) from the circle of Willis were surgically removed free of the posterior communicating and the basilar arteries.

2.3.2 | Skeletal muscle arteries

The general isolation procedure for the SEA has been previously described in detail [see[13] for video illustration]. Briefly, a ventral midline incision was made from the sternum to the pubis. While viewing through a stereo microscope, fat and connective tissue superficial to the sternum were removed to expose the proximal ends of the SEA. The abdominal muscle corresponding to the visible SEA was then removed and pinned ventral side facing up in the dissection chamber containing chilled dissection PSS. The SEA segment (~2 cm) was then dissected free of the paired vein, surrounding tissue and fat cells.

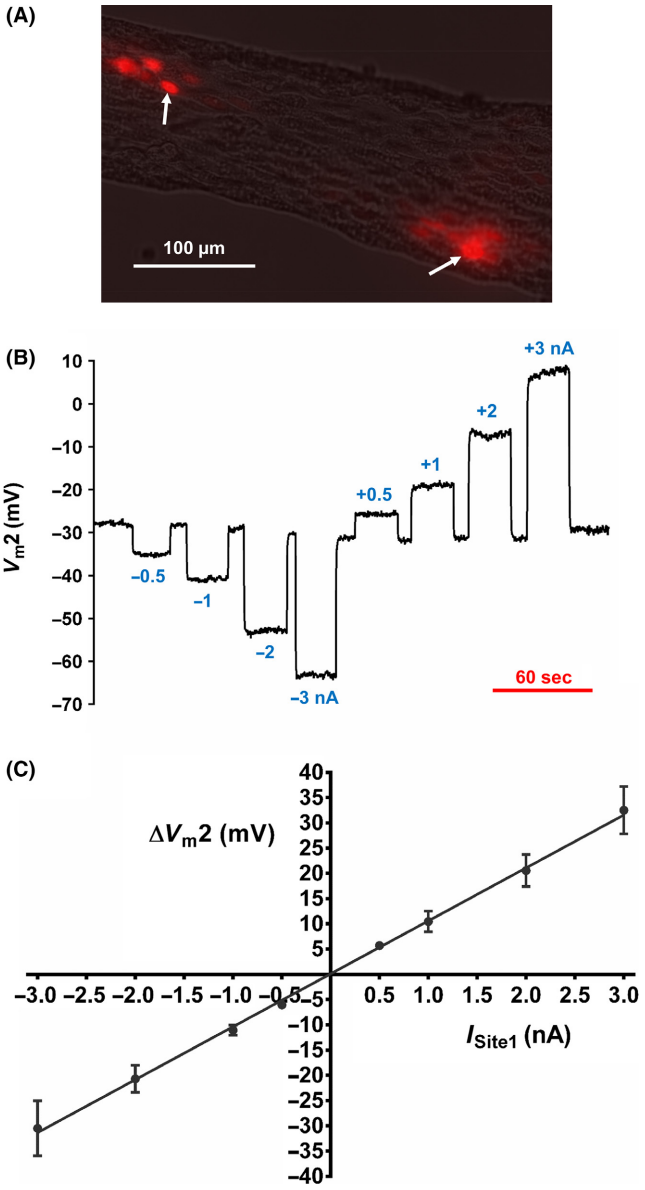

FIGURE 1 Freshly isolated cerebral arterial endothelium: evidence of dye transfer and electrical conduction. (A) Representative image following propidium iodide dye (0.1% in 2 mol·L^{-1} KCl) microinjection for ≥30 minutes into respective cells indicated by white arrows (separation distance = 250 µm). (B) Representative responses of V_m at Site 2 (V_m2; separation distance = 475 µm) to current pulses (±0.5-3 nA, ~20 sec each) injected at Site 1 to evoke progressive conducted hyperpolarization (from ~−5 to −30 mV) and depolarization (from ~+5 to +30 mV), respectively (separation distance = 475 µm). (C) Summary data for current injected into Site 1 vs ΔV_m at Site 2. Slope by linear regression ($R^2 \approx 1$) represents conduction amplitude = 10.5 ± 0.5 mV·nA^{-1} (n = 5, 2 male and 3 female; separation distance range, 250-500 µm)

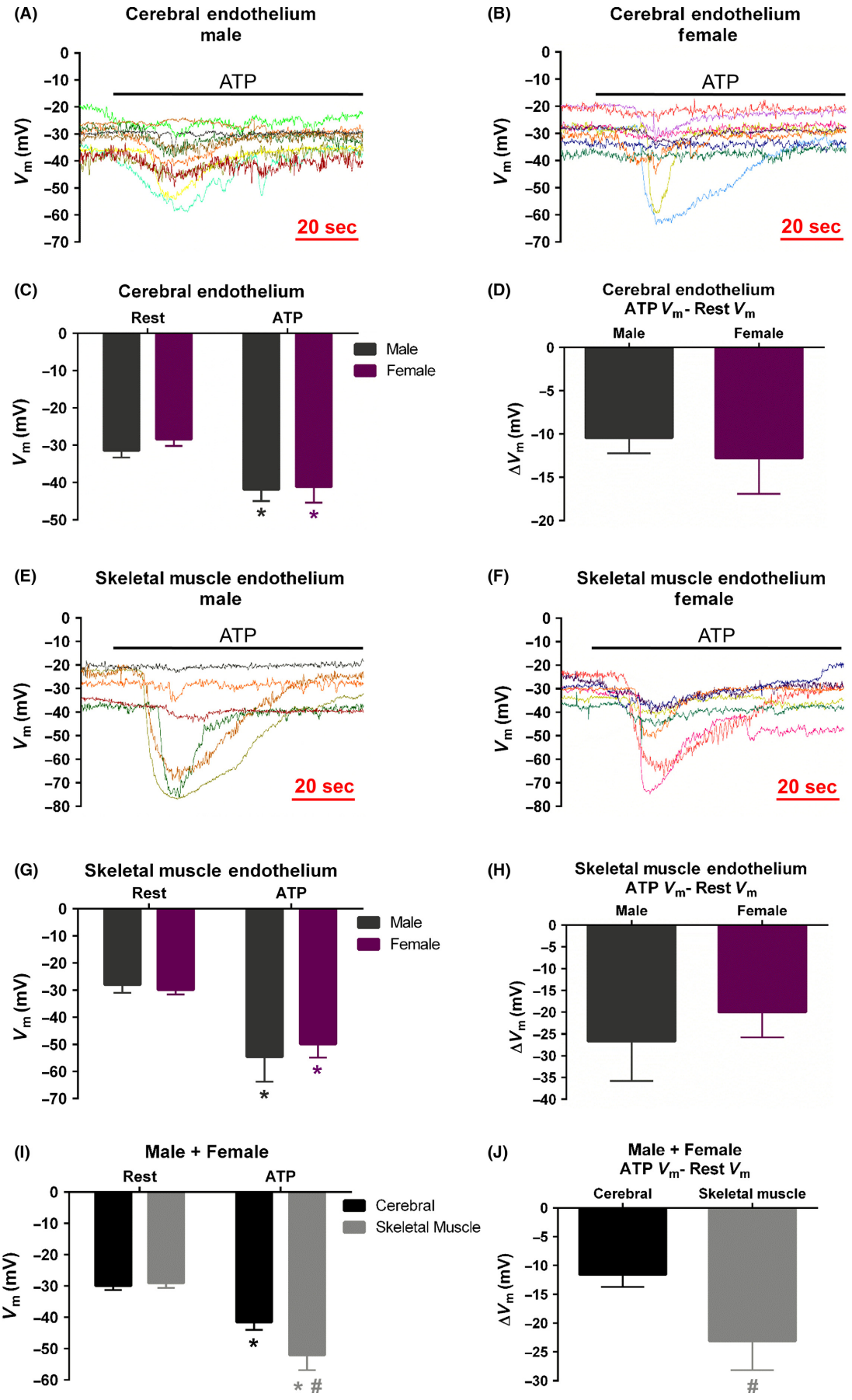
(A)
Cerebral endothelium male
ATP
20 sec
V_m (mV)
(B)
Cerebral endothelium female
ATP
20 sec
V_m (mV)
(C)
Cerebral endothelium
Rest
ATP
Male
Female
V_m (mV)
(D)
Cerebral endothelium
ATP V_m- Rest V_m
Male
Female
ΔV_m (mV)
(E)
Skeletal muscle endothelium male
ATP
20 sec
V_m (mV)
(F)
Skeletal muscle endothelium female
ATP
20 sec
V_m (mV)
(G)
Skeletal muscle endothelium
Rest
ATP
Male
Female
V_m (mV)
(H)
Skeletal muscle endothelium
ATP V_m- Rest V_m
Male
Female
ΔV_m (mV)
(I)
Male + Female
Rest
ATP
Cerebral
Skeletal Muscle
V_m (mV)
(J)
Male + Female
ATP V_m- Rest V_m
Cerebral
Skeletal muscle
ΔV_m (mV)

FIGURE 2 Adenosine triphosphate (ATP) stimulation of hyperpolarization in isolated endothelium of skeletal muscle and cerebral arteries. All panels illustrate V_m data before and during treatment with ATP (100 μmol·L^{-1}; purinergic receptor agonist and indirect SK_{Ca}/IK_{Ca} channel activator). *Cerebral endothelium:* Individual V_m traces in (A) male and female (B) mice. (C) Summary data of V_m before and during ATP treatment (peak hyperpolarization) in male and female endothelium. (D) As described in C for summary data of ΔV_m between peak hyperpolarization and resting V_m. Data indicate n = 10 (male) and n = 9 (female). *Skeletal muscle endothelium:* (E), (F), (G), and (H) are as described for A, B, C, and D, respectively, corresponding to skeletal muscle endothelium. Data indicate n = 6 (male) and n = 7 (female). *Cerebral* vs *skeletal muscle endothelium:* With both male and female groups included in each group, (I) reflects combined C and G and (J) reflects combined D and H. Data indicate n = 19 (cerebral) and n = 13 (skeletal muscle). Note that while differences between genders are not apparent in either type of endothelium, peak hyperpolarization during ATP treatment is greater in skeletal muscle endothelium vs cerebral. *Significantly different from paired resting V_m; #Significantly greater than ATP V_m and ΔV_m of unpaired cerebral endothelial tubes

2.4 | Endothelial tube isolation and superfusion

The apparatus for endothelial tube isolation included a modified Nikon inverted microscope (Ts2) equipped with phase contrast objectives (Ph1 DL; 10X & 20X) (Nikon Instruments Inc, Melville, NY, USA) and an aluminum stage (MXIX/AO; Siskiyou). An adjacent microsyringe pump controller [Micro4, World Precision Instruments (WPI), Sarasota, FL, USA] was used to isolate endothelium from surrounding adventitia and smooth muscle. The superfusion and experimental rig included a modified Nikon inverted microscope (Eclipse TS100) equipped with fluorescent objectives [20X (S-Fluor), and 40X (Plan Fluor)] and a manual aluminum stage (MXOP-SL, Siskiyou) mounted on a vibration isolation table (Micro-g; Technical Manufacturing, Peabody, MA, USA). For transferal between microscopes, a mobile tissue examination apparatus was used and included a Plexiglas superfusion chamber (RC-27; Warner Instruments, Camden, CT, USA) with a glass coverslip bottom (12-548-5M, Fisher; 2.4 × 5.0 cm) fastened into an anodized aluminum platform [PM6 or PH6 (diameter: 7.8 cm) & SA-NIK-AL (diameter: 10.8 cm), Warner Instruments)] that, in turn, was secured into a compact aluminum stage (8090P, Siskiyou, Grants Pass, OR, USA; length: 23 cm, width: 20 cm, thickness: 0.76 cm). All glass capillary tubes used for trituration of partially digested arteries and mechanical stabilization of isolated endothelial tubes were prepared using an electronic puller (P-97 or P-1000, Sutter Instruments, Novato, CA, USA) and a microforge (MF-900; Narishige, East Meadow, NY, USA) for heat polishing. Procedures for enzymatic isolation, securing isolated EC tubes, solution delivery, and temperature control are detailed below. The time elapsed from live animal to preparation of isolated endothelium ready for experimentation was less than 2 hours.

Intact arterial segments were cut into segments (length, 1-3 mm) and placed in a PSS containing 0.1 mmol·L^{-1} $CaCl_2$ and enzymes that dissociate intact endothelium from surrounding smooth muscle cells for a defined period of time (PCA: 10 minutes, SEA: 30 minutes) at 34°C. For PCAs, enzyme solution contained the following: 0.31 mg·mL^{-1} papain (P4762, Sigma), 0.5 mg·mL^{-1} dithioerythritol (D8255, Sigma), 0.75 mg·mL^{-1} collagenase (C8051, Sigma), and 0.13 mg·mL^{-1} elastase (E7885, Sigma). As previously described,[13] the SEA enzyme cocktail included 0.62 mg·mL^{-1} papain, 1.0 mg·mL^{-1} dithioerythritol, and 1.5 mg·mL^{-1} collagenase. Following partial digestion, each arterial segment was gently triturated to remove adventitia and smooth muscle cells using borosilicate glass capillary tubes [1B100-4, World Precision Instruments (WPI), Sarasota, FL, USA] with an internal tip diameter of 80-120 μm. Before every experiment, confirmation of an endothelial tube containing only endothelial cells was verified at 400× magnification.

Following EC isolation, a micromanipulator (MX10, Siskiyou) at each end of the mobile tissue examination platform held a micropipette with a blunted, spherical end (heat polished, OD: 100-150 μm; prepared from thin wall borosilicate glass (G150T-6, Warner Instruments)] to secure the endothelial tube against the bottom of the superfusion chamber. Continuous delivery of PSS (containing 2 mmol·L^{-1} $CaCl_2$) and respective drug solutions was ensured using a six-reservoir platform with valve controller (VC-6, Warner Instruments) and an inline flow control valve (FR-50, Warner Instruments). Temperature was continuously regulated using an inline heater (SH-27B, Warner Instruments) and heating platform (PM6 or PH6, Warner Instruments) coupled to a temperature controller (TC-344B, Warner Instruments). All experiments were performed during a flow rate of ~7-8 mL·min^{-1} with PSS (pH: 7.4, 37°C) as consistent with laminar flow while matching flow feed to vacuum suction and completed within 2 hours.

2.5 | Intracellular recording and intercellular coupling

The V_m of isolated endothelial tubes was recorded with Axoclamp 2B and Axoclamp 900A amplifiers (Molecular Devices, Sunnyvale, CA, USA) using microelectrodes pulled (P-97 or P-1000, Sutter Instruments) from glass capillary tubes (GC100F-10, Warner Instruments). Microelectrodes were backfilled with 2 M KCl (tip resistance: ~150 MΩ), whereas to test dye coupling, 0.1% propidium iodide (P4170, Sigma; mass, ~668 Da) dissolved in 2 mol·L^{-1} KCl was used to backfill microelectrodes. Cells were penetrated with microelectrodes while viewing the endothelial tube at 400X magnification. An Ag/AgCl pellet placed in the effluent PSS served as a reference electrode. Amplifier outputs were connected to a data acquisition system (Digidata 1550A, Molecular Devices) and audible baseline monitors (BM-A-TM, Ampol US LLC, Sarasota, FL, USA). For dual simultaneous intracellular recordings,[24] a cell was designated as "Site 1" using one electrode connected to the Axoclamp 2B amplifier driven by a function generator (FG-8002; EZ Digital, Seoul, South

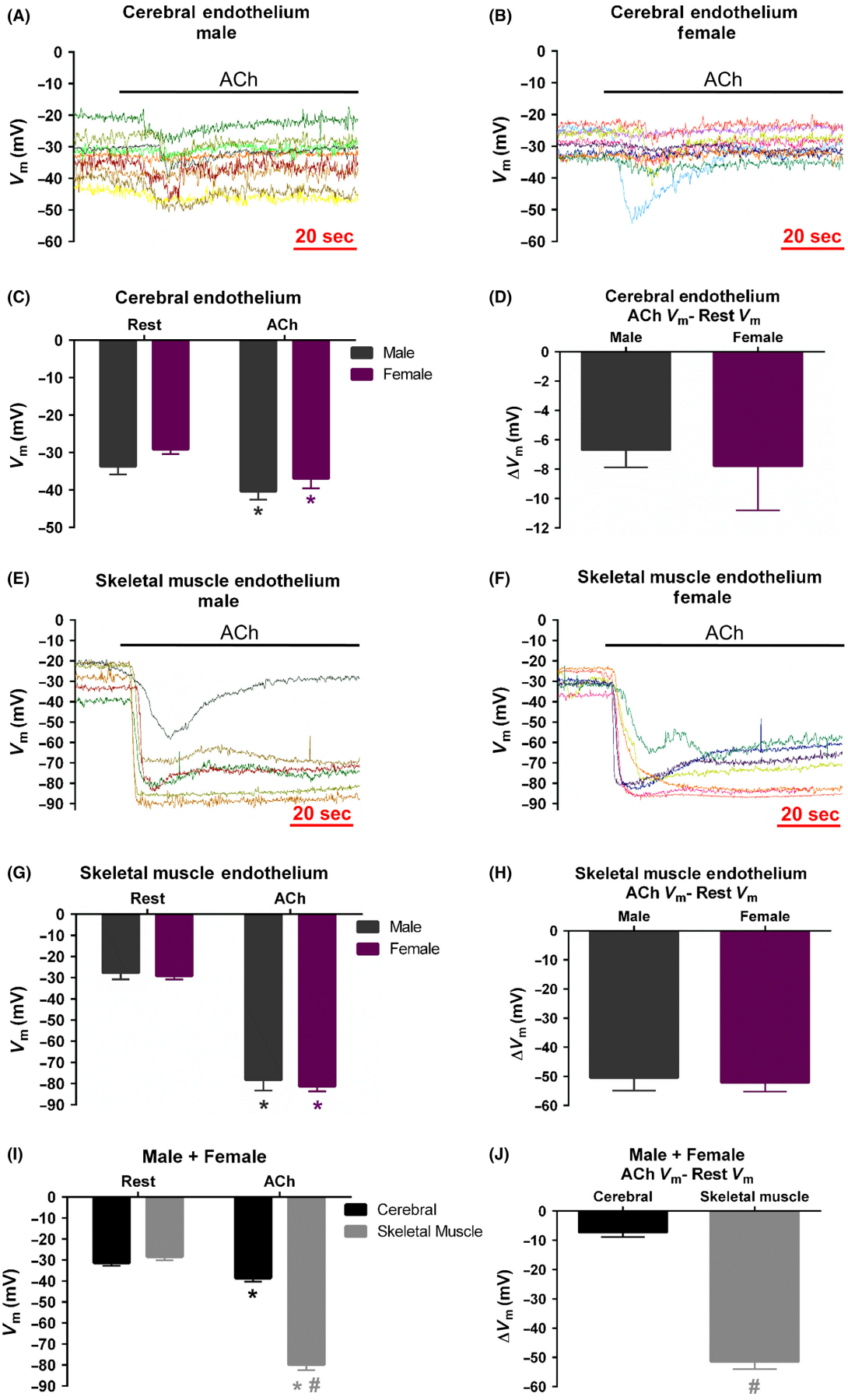
(A)
Cerebral endothelium male
ACh
20 sec
V_m (mV)
(B)
Cerebral endothelium female
ACh
20 sec
V_m (mV)
(C)
Cerebral endothelium
Rest
ACh
Male
Female
V_m (mV)
(D)
Cerebral endothelium
ACh V_m- Rest V_m
Male
Female
ΔV_m (mV)
(E)
Skeletal muscle endothelium male
ACh
20 sec
V_m (mV)
(F)
Skeletal muscle endothelium female
ACh
20 sec
V_m (mV)
(G)
Skeletal muscle endothelium
Rest
ACh
Male
Female
V_m (mV)
(H)
Skeletal muscle endothelium
ACh V_m- Rest V_m
Male
Female
ΔV_m (mV)
(I)
Male + Female
Rest
ACh
Cerebral
Skeletal Muscle
V_m (mV)
(J)
Male + Female
ACh V_m- Rest V_m
Cerebral
Skeletal muscle
ΔV_m (mV)

FIGURE 3 Acetylcholine (ACh) stimulation of hyperpolarization in isolated endothelium of skeletal muscle and cerebral arteries. All panels illustrate V_m data before and during treatment with ACh (10 μmol·L^{-1}; muscarinic receptor agonist and indirect SK_{Ca}/IK_{Ca} channel activator). *Cerebral endothelium:* Individual V_m traces in (A) male and female (B) mice. (C) Summary data of V_m before and during ACh treatment (peak hyperpolarization) in male and female endothelium. (D) As described in C for summary data of ΔV_m between peak hyperpolarization and resting V_m. Data indicate n = 9 (male) and n = 9 (female). *Skeletal muscle endothelium:* (E), (F), (G), and (H) are as described for A, B, C, and D, respectively, corresponding to skeletal muscle endothelium. Data indicate n = 6 (male) and n = 7 (female). *Cerebral* vs *skeletal muscle endothelium:* With both male and female groups included in each group, (I) reflects combined C and G and (J) reflects combined D and H. Data indicate n = 18 (cerebral) and n = 13 (skeletal muscle). Note that while differences between genders are not apparent in either type of endothelium, peak hyperpolarization during ACh treatment is greater in skeletal muscle endothelium vs cerebral. *Significantly different from paired resting V_m; #Significantly greater than ACh V_m and ΔV_m of unpaired cerebral endothelial tubes

Korea) and "Site 2" using another electrode connected to the Axoclamp 900A amplifier. For testing intercellular electrical coupling, current (±0.5-3 nA, ~20 second pulse duration) was delivered via the Axoclamp 2B amplifier at Site 1 against the direction of superfusion flow to Site 2 (distance: 250-500 μm).

Successful impalements were confirmed by sharp negative deflection of V_m, stable V_m for >1 min, reversible depolarization (≥20 mV) to 145 mmol·L^{-1} KCl, reversible hyperpolarization (≥−20 mV) to 1 μmol·L^{-1} NS309 (direct SK_{Ca}/IK_{Ca} channel opener, Tocris, Bristol, UK) and/or correspondence between current injection at Site 1 and V_m responses at Site 2. All data were acquired at 10 Hz on a Hewlett-Packard personal computer using Axoscope 10.5 software (Molecular Devices). Immediately following experiments with cerebral endothelial tubes whereby microelectrodes contained propidium iodide, images were acquired using a fluorescent microscope (Eclipse Ti-S; Nikon), a 60X objective [Plan Apo λ (numerical aperture: 0.95); Nikon), rhodamine filter set with solid state illumination (MIRA Light Engine; Lumencor, Inc., Beaverton, OR, USA), a 16-megapixel monochrome camera (DS-Qi2, Nikon), and Nikon imaging software (NIS Elements-F 4.60.00).

2.6 | Pharmacology

Adenosine 5′-triphosphate disodium salt hydrate (ATP, 100 μmol·L^{-1}; Sigma, A2383) and acetylcholine chloride (ACh, 10 μmol·L^{-1}; Sigma, A6625) were used independently to activate G-protein-coupled signaling through purinergic (P2Y type) or muscarinic (M_3 type) receptors, respectively, which, in arterial ECs, activate Ca^{2+} release through IP_3 receptors and Ca^{2+} influx via TRP channels to activate SK_{Ca}/IK_{Ca} channels.[1,22] NS309 (0.01-10 μmol·L^{-1}; Tocris, Bristol, UK, 3895) was applied to directly evaluate the capacity for SK_{Ca}/IK_{Ca} channel-dependent hyperpolarization.[22,24] Extracellular KCl ($[K^+]_o$) elevated to 15 mmol·L^{-1} was used to examine the presence of hyperpolarization to K_{IR} channel activation; a subset of experiments employed 15 mmol·L^{-1} KCl in combination with $BaCl_2$ (100 μmol·L^{-1}; K_{IR} channel block).[25,26]

A stable resting V_m of >1 minute was allowed before application of a pharmacological agent, whereby each application was ≥3 minutes as needed to allow for records of stable peak V_m responses. In the case of NS309 concentration-response determinations, washout with control PSS to baseline conditions was applied between each concentration before the next concentration was added.[24,27] ATP, ACh, and $BaCl_2$ were prepared in PSS, whereas NS309 was dissolved in DMSO (final working concentration ≤1%). Pharmacological agents were added to the superfusion solution, thereby exposing the entire endothelial tube to each agent.

2.7 | Data and statistical analysis

The data and statistical analysis comply with the recommendations on experimental design and analysis in pharmacology.[28] Differences between groups were accepted as statistically significant with $P < .05$. Summary data are presented as means ± SE, and n represents the number of independent experiments using one endothelial tube from a different mouse for a given experimental protocol. Typically, each experimental procedure required ≥5 mice for a complete dataset in accord with statistical power analysis ($\alpha = 0.05$, power = 0.80). In the case of intracellular recordings, data analyses included (1) resting V_m (mV) and (2) change in V_m (ΔV_m) = peak response V_m—preceding baseline V_m. Statistical analysis was performed using GraphPad Prism (version 6.07; GraphPad Software, La Jolla, CA, USA) and analyses included linear regression (ΔV_m at "Site 2" vs current injection at "Site 1"; $R^2 \geq 0.99$), curve fitting [concentration responses for pEC_{50} determinations; sigmoidal "log (agonist) vs response with variable slope" fit, $R^2 \geq 0.99$], and unpaired (across gender and/or endothelial type) and paired (drug response vs resting V_m in same endothelial tube) *t*-tests.

3 | RESULTS

Endothelial tubes isolated from posterior cerebral and superior epigastric arteries were ~90-100 μm and ~60-70 μm in width, respectively, whereby arterial segments used for this study were typically between 0.5 and 1 mm in length. The mechanical stability of secured, isolated endothelium enabled continuous intracellular recordings of V_m lasting typically up to 2 hours at 37°C. Resting V_m was similar across cerebral (−30 ± 1 mV, n = 19) and skeletal muscle (−29 ± 2 mV, n = 13) endothelial tubes. The Results below qualitatively denote comparisons across respective types of endothelium and genders, whereby quantitative information (eg, n-values and means ± SE) supporting general descriptions of observations is indicated in the Figures and Figure Legends.

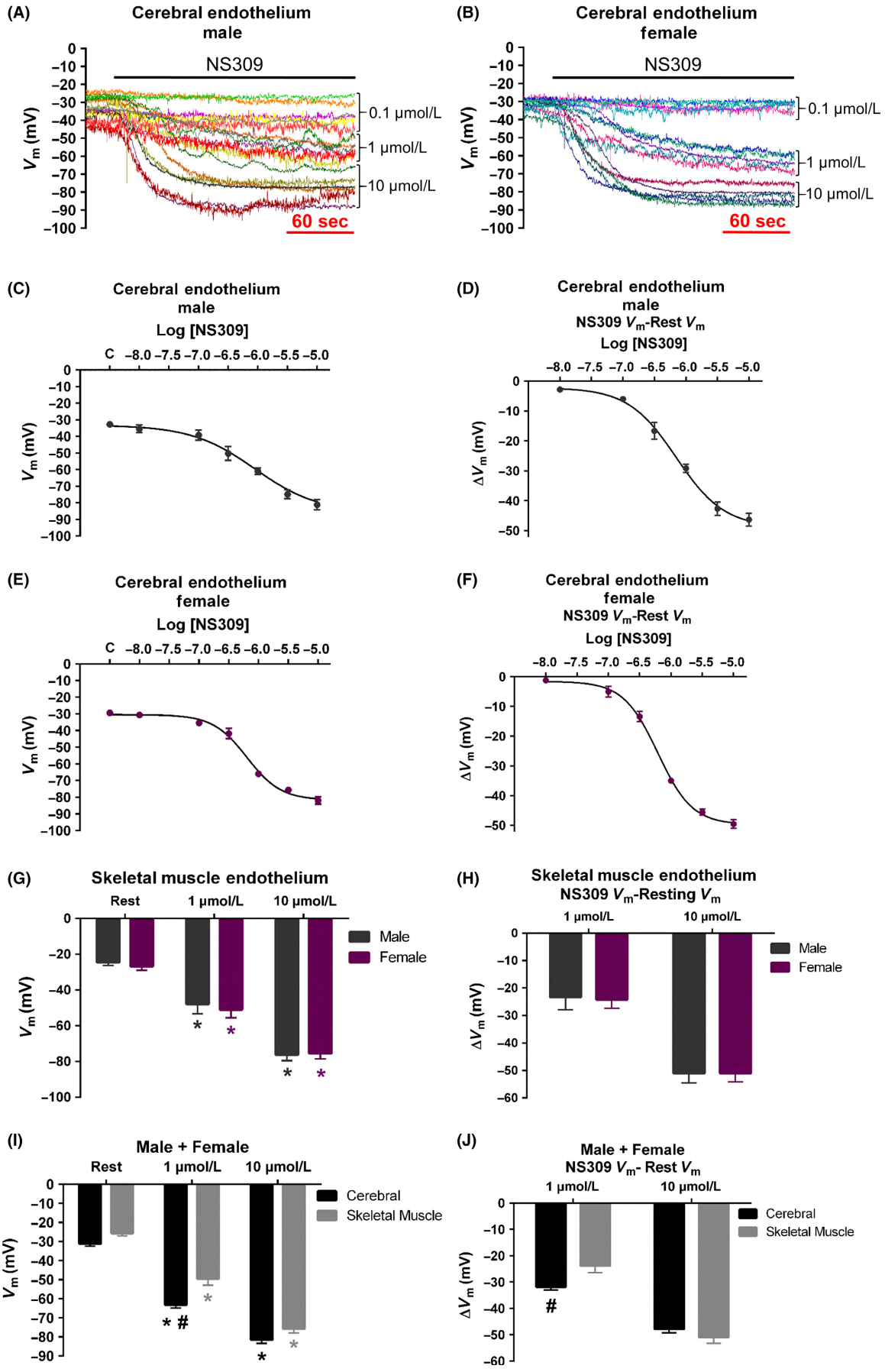
(A)
Cerebral endothelium
male
NS309
0.1 µmol/L
1 µmol/L
10 µmol/L
60 sec
V_m (mV)
(B)
Cerebral endothelium
female
NS309
0.1 µmol/L
1 µmol/L
10 µmol/L
60 sec
V_m (mV)
(C)
Cerebral endothelium
male
Log [NS309]
C –8.0 –7.5 –7.0 –6.5 –6.0 –5.5 –5.0
V_m (mV)
(D)
Cerebral endothelium
male
NS309 V_m-Rest V_m
Log [NS309]
–8.0 –7.5 –7.0 –6.5 –6.0 –5.5 –5.0
ΔV_m (mV)
(E)
Cerebral endothelium
female
Log [NS309]
C –8.0 –7.5 –7.0 –6.5 –6.0 –5.5 –5.0
V_m (mV)
(F)
Cerebral endothelium
female
NS309 V_m-Rest V_m
Log [NS309]
–8.0 –7.5 –7.0 –6.5 –6.0 –5.5 –5.0
ΔV_m (mV)
(G)
Skeletal muscle endothelium
Rest
1 µmol/L
10 µmol/L
Male
Female
V_m (mV)
(H)
Skeletal muscle endothelium
NS309 V_m-Resting V_m
1 µmol/L
10 µmol/L
Male
Female
ΔV_m (mV)
(I)
Male + Female
Rest
1 µmol/L
10 µmol/L
Cerebral
Skeletal Muscle
V_m (mV)
(J)
Male + Female
NS309 V_m- Rest V_m
1 µmol/L
10 µmol/L
Cerebral
Skeletal Muscle
ΔV_m (mV)

FIGURE 4 NS309 stimulation of hyperpolarization in isolated endothelium of skeletal muscle and cerebral arteries. All panels illustrate V_m data before and during treatment with NS309 (0.1-10 $\mu mol \cdot L^{-1}$; direct SK_{Ca}/IK_{Ca} channel activator). *Cerebral endothelium:* Individual V_m traces in (A) male and female (B) mice. (C) Summary data of V_m before and during progressive NS309 treatment (peak hyperpolarization during each [NS309]) in male endothelium. (D) As described in C for summary data of ΔV_m between peak hyperpolarization and resting V_m. (E) and (F) are as described for C and D, respectively, for female. Respective pEC_{50}s and maximal hyperpolarization responses are (D) 6.18 ± 0.06, ΔV_m: −46 ± 2 mV and (F) 6.22 ± 0.04, ΔV_m: −50 ± 2. Data indicate n = 6 (male) and n = 5 (female). *Skeletal muscle endothelium:* (G) Summary data of V_m before and during peak hyperpolarization to NS309 (1 and 10 $\mu mol \cdot L^{-1}$) in male and female endothelium. (H) As described in G for summary data of ΔV_m between peak hyperpolarization and resting V_m. Data indicate n = 6 (male) and n = 7 (female). *Cerebral* vs *skeletal muscle endothelium:* With both male and female groups included in each group, (I) reflects combined C, E, and G and (J) reflects combined D, F, and H [resting and NS309 (1 and 10 $\mu mol \cdot L^{-1}$)]. Data indicate n = 11 (cerebral) and n = 13 (skeletal muscle). Note that hyperpolarization to NS309 is preserved across both types of endothelial tubes and respective genders. *Significantly different from paired resting V_m; #Significantly greater than NS309 (1 $\mu mol \cdot L^{-1}$) V_m and ΔV_m of unpaired skeletal muscle endothelial tubes

3.1 | Freshly isolated cerebral endothelium: Evidence of cell-to-cell coupling and electrical conduction

Cell-to-cell coupling through gap junctions has been observed in isolated endothelial tubes of skeletal muscle using visual and electrical approaches of microinjected propidium iodide dye and current injection via dual intracellular electrodes, respectively.[24,27] As illustrated in Figure 1, the presence of dye transfer also occurs in cerebral endothelial tubes (Figure 1A), while using current injections of ±0.5-3 nA (Figure 1B), ΔV_m responses were linear throughout and reflected a ~10-11 mV change per nA of current injected (250-500 μm from the site of current injection; Figure 1C). These data illustrate an intact cerebral endothelial tube system whereby cells are coupled through gap junctions. These observations demonstrating robust dye transfer and conduction amplitude measurements in cerebral endothelium are similar to skeletal muscle endothelium as shown in previous studies.[24,27,29]

3.2 | Hyperpolarization of cerebral and skeletal muscle endothelium to indirect and direct activation of SK_{Ca}/IK_{Ca} channels

Significant hyperpolarization of V_m (≥5 mV) occurred in endothelial tubes of cerebral and skeletal muscle arteries in response to the classical endothelial GPCR agonists ATP (Figure 2) and ACh (Figure 3) as indirect activators of SK_{Ca}/IK_{Ca} channels.[1,22] As illustrated in Figure 2 (Panels A and B & E and F), hyperpolarization to ATP was typically transient (≤30 seconds) throughout individual V_m recordings. With similar responses observed across genders for respective types of endothelial tubes (Figure 2C and D & G and H), peak hyperpolarization to ATP in skeletal muscle endothelial cells was ~twofold greater vs cerebral endothelial cells (Figures 2I and J). In skeletal muscle endothelial tubes only, hyperpolarization responses to ACh were sustained throughout duration of treatment (compare Figure 3 panels A and B with E and F). With similar responses observed across genders for respective types of endothelial tubes (Figure 3C and D & G and H), peak hyperpolarization to ACh in skeletal muscle endothelia was ~sevenfold greater vs cerebral endothelial tubes (Figures 3I and J).

Direct activation of SK_{Ca}/IK_{Ca} channels with NS309 can fine tune V_m from steady-state conditions in the absence of agonist exposure (or "resting" V_m) to the equilibrium potential for K^+ (~−90 mV).[24,27] Figures 4A & B illustrate sustained hyperpolarization responses in individual cerebral endothelial tubes to "low" (0.1 $\mu mol \cdot L^{-1}$), "middle" (1 $\mu mol \cdot L^{-1}$), and "high" (10 $\mu mol \cdot L^{-1}$) concentrations of NS309 for males and females, respectively. Summary concentration response curves to NS309 (resting V_m to maximum V_m during 10 $\mu mol \cdot L^{-1}$) indicate a similarity across genders with regard to respective pEC_{50}s and maximal hyperpolarization (Figure 4C-F). Such experiments have been performed previously for male skeletal muscle endothelial tubes[24] and thus, in this regard, comparisons are only indicated for effective concentrations of 1 $\mu mol \cdot L^{-1}$ and 10 $\mu mol \cdot L^{-1}$ NS309. Robust hyperpolarization to NS309 (ΔV_m > -20 mV) for skeletal muscle endothelial tubes was preserved across genders (Figure 4G and H) as well as in comparison to cerebral endothelial tubes (Figure 4I and J).

3.3 | Hyperpolarization of cerebral endothelium to activation of K_{IR} channels

Elevated $[K^+]_o$ (15 $mmol \cdot L^{-1}$ KCl) stimulates activation of K_{IR} channels in arteries of the brain[26] and skeletal muscle.[25] Significant hyperpolarization of V_m (≥5 mV) occurred in response to 15 $mmol \cdot L^{-1}$ KCl in endothelial tubes of cerebral vessels (Figure 5A-D) but not skeletal muscle (Figure 5E-H). With similar responses observed across genders for respective types of endothelium (Figure 5C and D & G and H), peak hyperpolarization to 15 $mmol \cdot L^{-1}$ KCl in cerebral endothelial tubes averaged ΔV_m ~7-8 mV. However, ΔV_m responses in skeletal muscle during 15 $mmol \cdot L^{-1}$ KCl were indistinguishable from those observed in cerebral endothelial tubes during K_{IR} blockade with a combined treatment using $BaCl_2$ (100 $\mu mol \cdot L^{-1}$) and 15 $mmol \cdot L^{-1}$ KCl (Figures 5I-J).

4 | DISCUSSION

The endothelial layer of resistance arteries contributes to regulation of peripheral skeletal muscle and cerebrovascular smooth muscle tone and thereby modulates optimal blood flow ensuring a constant

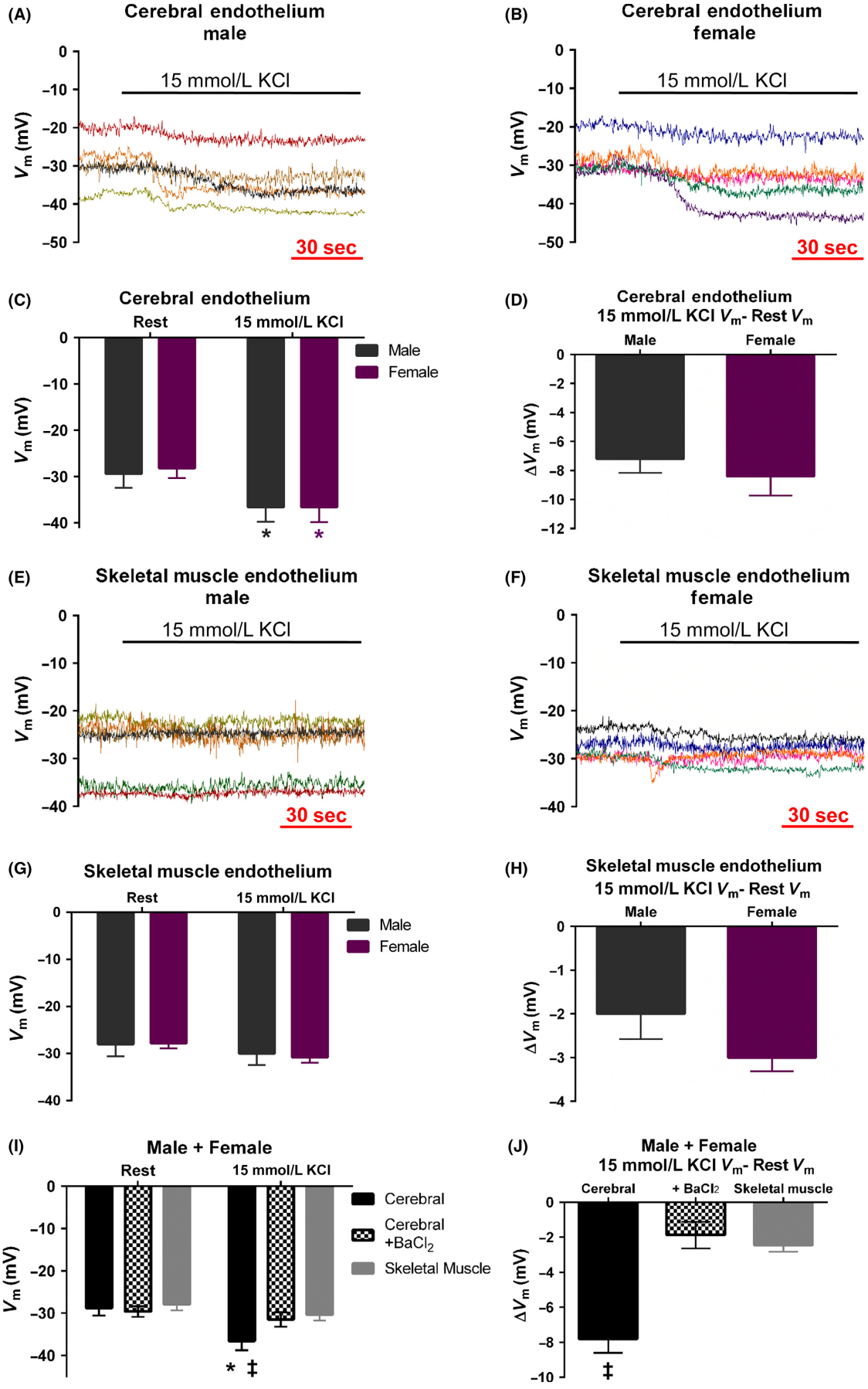
(A)
Cerebral endothelium male
15 mmol/L KCl
30 sec
V_m (mV)
(B)
Cerebral endothelium female
15 mmol/L KCl
30 sec
V_m (mV)
(C)
Cerebral endothelium
Rest
15 mmol/L KCl
Male
Female
V_m (mV)
(D)
Cerebral endothelium
15 mmol/L KCl V_m- Rest V_m
Male
Female
ΔV_m (mV)
(E)
Skeletal muscle endothelium male
15 mmol/L KCl
30 sec
V_m (mV)
(F)
Skeletal muscle endothelium female
15 mmol/L KCl
30 sec
V_m (mV)
(G)
Skeletal muscle endothelium
Rest
15 mmol/L KCl
Male
Female
V_m (mV)
(H)
Skeletal muscle endothelium
15 mmol/L KCl V_m- Rest V_m
Male
Female
ΔV_m (mV)
(I)
Male + Female
Rest
15 mmol/L KCl
Cerebral
Cerebral +$BaCl_2$
Skeletal Muscle
V_m (mV)
(J)
Male + Female
15 mmol/L KCl V_m- Rest V_m
Cerebral
+ $BaCl_2$
Skeletal muscle
ΔV_m (mV)

FIGURE 5 15 mmol·L^{-1} $[K^+]_o$ stimulation of hyperpolarization in isolated endothelium of skeletal muscle and cerebral arteries. All panels illustrate V_m data before and during treatment with 15 mmol·L^{-1} KCl (K_{IR} channel activator). *Cerebral endothelium:* Individual V_m traces in (A) male and female (B) mice. (C) Summary data of V_m before and during 15 mmol·L^{-1} KCl treatment (peak hyperpolarization) in male and female endothelium. (D) As described in C for summary data of ΔV_m between peak hyperpolarization and resting V_m. Data indicate n = 5 (male) and n = 5 (female). *Skeletal muscle endothelium:* (E), (F), (G), and (H) are as described for A, B, C, and D, respectively, corresponding to skeletal muscle endothelium. Data indicate n = 6 (male) and n = 5 (female). *Cerebral vs skeletal muscle endothelium:* With both male and female genders included in each group and block of K_{IR} channels in cerebral endothelial tubes with $BaCl_2$ (100 μmol·L^{-1}) included, (I) reflects combined C and G and (J) reflects combined D and H. Data indicate n = 10 (cerebral), n = 8 (cerebral 15 mmol·L^{-1} KCl + $BaCl_2$; 4 male and 4 female) and n = 11 (skeletal muscle). Pretreatment with $BaCl_2$ alone did not have a significant effect on V_m (Resting: −32 ± 2 mV, $BaCl_2$: −31 ± 2 mV). Note that hyperpolarization in response to 15 mmol·L^{-1} KCl is negligible in skeletal muscle vs cerebral endothelial tubes regardless of gender. *Significantly different from paired resting V_m; ‡Significantly greater than V_m and ΔV_m of cerebral 15 mmol·L^{-1} KCl + $BaCl_2$ and skeletal muscle + 15 mmol·L^{-1} KCl

delivery of oxygen and nutrients to excitable tissues.[30] Our understanding of endothelial function has been enhanced with the use of a skeletal muscle arterial endothelial tube study model containing cells coupled via gap junctions in the absence of perivascular nerves and smooth muscle. Using this study model, we have been able to resolve electrical signaling dynamics disparate from "excitable" cells such as neurons and cardiac myocytes[31] while illuminating refined pharmacological approaches for controlling cardiovascular function.[12] With recognition of recent demonstrations of how the endothelium plays an important role in modulating moment to moment vascular tone and blood flow within the brain,[3,32] we utilized the endothelial tube model to investigate purinergic and muscarinic receptor stimulation in mouse cerebral arteries relative to skeletal muscle arteries. To our knowledge, this study has comprehensively measured hyperpolarizing electrical dynamics in freshly isolated and intact cerebral arterial endothelial tubes (see Figure 1) of male and female mice for the first time. We found that although GPCR-triggered hyperpolarization responses in cerebral endothelium were modest relative to skeletal muscle, robust SK_{Ca}/IK_{Ca} and K_{IR} channel functions were present. We did not observe statistically significant differences across respective genders. Our findings are discussed below in the context of physiological integration of central vs peripheral distribution of blood flow with implications for treatment of cardio/cerebrovascular diseases.

4.1 | Physiological integration: Role of endothelial purinergic and muscarinic signaling

Along with noradrenaline, ATP can be released from perivascular sympathetic nerves that enmesh cerebral and skeletal muscle arteries.[33] Actions of ATP are biphasic whereby activation of P2X receptors evokes constriction (alone or in combination of noradrenaline activation of smooth muscle α_1-adrenoreceptors) followed by smooth muscle relaxation via EDH resulting from activation of endothelial P2Y receptors.[34,35] Although its effects are more straightforward for evoking endothelial M_3 receptors and downstream hyperpolarization (vs ATP), the source of ACh is controversial and may include excess ACh "spillover" from neuromuscular junctions during skeletal muscle contraction,[36] cholinergic sympathetic dilator nerves surrounding skeletal muscle blood vessels of experimental animal models,[37] and/or the endothelium itself.[38] Regardless, we simplified our investigation here with examining EDH responses to ATP and ACh using freshly isolated endothelium and found that peak hyperpolarization was, respectively, ~twofold and ~sevenfold higher in skeletal muscle vs cerebral vascular endothelial tubes (Figures 2 and 3). These findings were not surprising as vascular resistance networks of skeletal muscle engage in "functional sympatholysis",[39] a process that requires rapid endothelial activation and production of vasodilation to counteract the basal activation of smooth muscle α_1-adrenoreceptors along resistance networks in accord with metabolic demand.[30] On the contrary, blood flow distribution to the brain is relatively constant throughout conditions of rest and exercise[15] as the variable metabolic demands by neurons are typically met by alterations in cerebral blood flow governed by myogenic autoregulation that operates over a wide systolic pressure range of ~60-140 mmHg.[40]

4.2 | Endothelial K_{Ca} and K_{IR} channels

The endothelial SK_{Ca}/IK_{Ca} channels have been recognized for their integral role during blood flow to the brain[3,41] and skeletal muscle.[12,30] Despite the differential hyperpolarization to ATP and ACh across organs, SK_{Ca}/IK_{Ca} channel activation and hyperpolarization to NS309 in cerebral endothelium (up to ~−80 mV) was remarkably similar to skeletal muscle endothelium regardless of gender (Figure 4). These data indicate that the capacity of SK_{Ca}/IK_{Ca} channel activity is independent of hormonal or neurotransmitter activation of GPCRs. Similar to skeletal muscle blood flow, modulation of cerebral blood flow as influenced by endothelial SK_{Ca}/IK_{Ca} channels may be susceptible to posttranslational activity such as oxidative signaling.[12]

Although studied primarily in smooth muscle, endothelial $K_{IR}2.1$ channels are present in the endothelium of rodent resistance arteries and arterioles.[42] In agreement with recent studies,[22,43] our findings here using isolated cerebral endothelium indicate consistent hyperpolarization responses to 15 mmol·L^{-1} KCl (Figure 5A-D). Also, the apparent lack of endothelial K_{IR} function in SEAs (Figure 5E-H) is consistent with recent observations, whereby K_{IR} channels play a dominant role in the smooth muscle layer in young (3-6 month) mice despite detectable mRNA expression of endothelial $K_{IR}2.1$ in both cell layers.[25] In contrast to skeletal muscle, K_{IR} channel currents have

been observed in the endothelium but not in the smooth muscle of rodent mesenteric arteries.[44] Thus, whereas both peripheral and central types of endothelium rely on SK_{Ca}/IK_{Ca} channels to generate vasodilatory hyperpolarization, only cerebral vessels may contain functional K_{IR} channels in both smooth muscle and endothelium to sense $[K^+]_o$ as a metabolic byproduct to intimately match cerebral blood flow with neuronal metabolism.[45] The dual presence of K_{IR} channels in cerebral smooth muscle and endothelium produces a higher magnitude of vascular hyperpolarization (>20 mV vs <10 mV in this study using cerebral endothelium alone) as K^+ efflux through activated endothelial SK_{Ca}/IK_{Ca} channels raises $[K^+]_o$ to further stimulate smooth muscle K_{IR} channels.[3,43] Altogether, the presence and interaction of endothelial K_{IR} and SK_{Ca}/IK_{Ca} channels should be considered for understanding and therapeutically addressing the loss of cerebrovascular autoregulation during disease conditions such as stroke.[17,26]

4.3 | Lack of gender-related differences in young mice

We prioritized the inclusion of both genders in this study as ≥80% of biomedical studies thus far have focused on males only[46] and have thereby neglected 50% of the sample population. We did not find statistically significant differences across males and females for respective central and peripheral vascular endothelial systems. However, we do not exclude the possibility of gender-related differences emerging with advanced age and associated vascular diseases related to enhancement of oxidative signaling.[12] Indeed, hypertension induced via global knockdown of endothelial NO synthase and Cyclooxygenase-1 (components of parallel endothelial vasodilator pathways to EDH) has been found to have a minimal effect on vascular tone of mesenteric arteries and systolic blood pressure in female vs male mice.[47] Although, these transgenic interventions were not specific to vascular endothelium and thus, there are several other confounding factors regarding relationships between central vs peripheral arteries and regulation of vascular tone via perivascular nerves vs smooth muscle vs endothelium. Regardless of previous efforts, our current electrophysiological findings suggest that endothelial function of central and peripheral arteries of young adult C57BL/6 mice is similar across males and females. Perhaps either gender can be used for future studies of endothelial function in young adult animals as consistent with the "reduction" component of the 3Rs (replacement, refinement, and reduction) of experimental animal use and care.

4.4 | Use of the isolated endothelial tube model and lack of myoendothelial coupling

Coordination of vascular smooth muscle and endothelium to govern vascular tone and resistance has been demonstrated through mechanisms collectively known as "myoendothelial coupling". An original investigation resolved the presence and structure of myoendothelial gap junctions that facilitate transmission of electrical signals between endothelium and smooth muscle in rat mesenteric arteries.[48] Altogether, several studies over the past ~20 years have employed use of confocal and electron microscopic examination of isolated arteries (eg, of the gut, cremaster, and brain). As a result, an emerging working paradigm currently illustrates that endothelial projections through the internal elastic lamina contain a "microdomain" of spatially proximal myoendothelial gap junctions, IK_{Ca} channels, transient receptor potential channels (eg, vanilloid class, TRPV4), and inositol 1,4,5-trisphosphate receptors (or IP_3Rs).[49-52] Either myoendothelial or endothelial gap junctions may contain connexins (or Cxns) 37, 40, and/or 43 with SK_{Ca} channels primarily localized near endothelial gap junctions only.[50] Regardless, as demonstrated by this study and others where such a microdomain is eliminated,[12] components of endothelial $[Ca^{2+}]_i$ regulation (influx and intracellular release), maintenance of V_m, hyperpolarization of V_m (up to E_K) via SK_{Ca}/IK_{Ca} activation, and intercellular coupling via gap junctions are retained. Although, we recognize that blood flow is not governed by either smooth muscle or endothelium alone. Indeed, the experimental strengths of the endothelial tube study model are also its physiological limitations with respect to the lack of perivascular nerves, smooth muscle, circulation of blood, and hormonal regulation.[12] For balanced consideration among use of physiological study models, there are also significant limitations for experimental applications in vivo (eg, inflammation, artifacts of anesthesia) and ex vivo (eg, detachment from parenchyma, lack of blood flow) [reviewed for the brain in[53]]. Our goal of this study was to address contrasting electrical dynamics of endothelium of cerebral and skeletal muscle resistance arteries. Our findings are complementary to previous intact PCA and SEA studies where myoendothelial communication was present.[22,25,43] In turn, our data highlight use of freshly intact endothelium isolated from male and female mouse cerebral arteries for the first time.

5 | SUMMARY AND CONCLUSIONS: TRANSLATIONAL PERSPECTIVE

The primary significance of this study is that despite weaker hyperpolarization in response to endothelial GPCR stimulation in cerebral vs skeletal muscle endothelium, the capability for robust SK_{Ca}/IK_{Ca} activity is preserved across brain and skeletal muscle regardless of gender. Furthermore, we are now confident that functionally active K_{IR} channels are present in intact cerebral arterial endothelium, but lacking in skeletal muscle arterial endothelium. The activity of SK_{Ca}/IK_{Ca} channels underlies EDH and is amenable to "fine-tuning" with use of agents such as NS309 and SKA-31.[27] While staying within physiological limits as previously discussed [eg, not exceeding a stable V_m of ~−60 mV[12]], mild SK_{Ca}/IK_{Ca} channel activation may also serve as a feed-forward mechanism to enhance Ca^{2+} entry to further amplify SK_{Ca}/IK_{Ca} channel activity[5] and/or boost production of NO.[9,10,54] As endothelial-derived relaxation decreases in old age[55] and diseases such as hypertension,[56] sleep apnea[57] and obesity[58] due to reduced nitric oxide signaling, SK_{Ca}/IK_{Ca} channel activity may be calibrated as needed to restore blood flow demands to respective organs.[12] Altogether, these data provide fundamentally new insight

for precision medicine, whereby selective treatments may be developed for key vascular biomarkers and their function across organ systems in order to promote health and prevent vascular disease.

ACKNOWLEDGEMENTS

Charles Hewitt provided excellent technical assistance with establishment of the Behringer laboratory with key equipment (eg, microdissection stations, microscopes, cameras, and endothelium isolation and electrophysiological apparati). We also thank LLU Campus Engineering for assistance with building custom stainless steel dissection chambers and electrophysiology accessories. Lastly, we acknowledge charitable contributions of a Nikon TS100 microscope and an Axoclamp 2B electrometer by Drs. Sean M. Wilson and Christopher G. Wilson, respectively, of the LLU Center for Perinatal Biology.

This research was supported by Loma Linda University School of Medicine new faculty start-up funds and National Institutes of Health grant R00-AG047198R0 (EJB). The content of this article is solely the responsibility of the authors and does not necessarily represent the official views of the National Institutes of Health.

AUTHOR CONTRIBUTIONS

MAH and EJB designed and/or performed experiments in the laboratory of EJB. MAH, JNB, and EJB analyzed and interpreted data. MAH, JNB, and EJB drafted the manuscript and/or prepared the figures. MAH, JNB, and EJB edited the manuscript. All authors approved the final version of the manuscript and agree to be accountable for all aspects of the work in ensuring that questions related to the accuracy or integrity of any part of the work are appropriately investigated and resolved. All persons designated as authors qualify for authorship, and all those who qualify for authorship are listed.

DISCLOSURES

The authors declare no conflicts of interest.

ORCID

Md A. Hakim http://orcid.org/0000-0002-6183-7950
John N. Buchholz http://orcid.org/0000-0002-8356-3831
Erik J. Behringer http://orcid.org/0000-0001-6979-2796

REFERENCES

1. Busse R, Edwards G, Feletou M, Fleming I, Vanhoutte PM, Weston AH. EDHF: bringing the concepts together. *Trends Pharmacol Sci*. 2002;23:374-380.
2. Garland CJ, Dora KA. EDH: endothelium-dependent hyperpolarization and microvascular signaling. *Acta Physiol (Oxf)*. 2017;219:152-161.
3. Longden TA, Dabertrand F, Koide M, et al. Capillary K^+-sensing initiates retrograde hyperpolarization to increase local cerebral blood flow. *Nat Neurosci*. 2017;20:717-726.
4. Ledoux J, Werner ME, Brayden JE, Nelson MT. Calcium-activated potassium channels and the regulation of vascular tone. *Physiology (Bethesda)*. 2006;21:69-78.
5. Behringer EJ, Segal SS. Membrane potential governs calcium influx into microvascular endothelium: integral role for muscarinic receptor activation. *J Physiol*. 2015;593:4531-4548.
6. Busse R, Fichtner H, Luckhoff A, Kohlhardt M. Hyperpolarization and increased free calcium in acetylcholine-stimulated endothelial cells. *Am J Physiol Heart Circ Physiol*. 1988;255:H965-H969.
7. Busse R, Mulsch A. Calcium-dependent nitric oxide synthesis in endothelial cytosol is mediated by calmodulin. *FEBS Lett*. 1990;265:133-136.
8. Garland CJ, Plane F, Kemp BK, Cocks TM. Endothelium-dependent hyperpolarization: a role in the control of vascular tone. *Trends Pharmacol Sci*. 1995;16:23-30.
9. Dalsgaard T, Kroigaard C, Misfeldt M, Bek T, Simonsen U. Openers of small conductance calcium-activated potassium channels selectively enhance NO-mediated bradykinin vasodilatation in porcine retinal arterioles. *Br J Pharmacol*. 2010;160:1496-1508.
10. Stankevicius E, Dalsgaard T, Kroigaard C, et al. Opening of small and intermediate calcium-activated potassium channels induces relaxation mainly mediated by nitric-oxide release in large arteries and endothelium-derived hyperpolarizing factor in small arteries from rat. *J Pharmacol Exp Ther*. 2011;339:842-850.
11. Wulff H, Kohler R. Endothelial small-conductance and intermediate-conductance K_{Ca} channels: an update on their pharmacology and usefulness as cardiovascular targets. *J Cardiovasc Pharmacol*. 2013;61:102-112.
12. Behringer EJ. Calcium and electrical signaling in arterial endothelial tubes: new insights into cellular physiology and cardiovascular function. *Microcirculation* 2017;24:1-12.
13. Socha MJ, Segal SS. Isolation of microvascular endothelial tubes from mouse resistance arteries. *J Vis Exp* 2013;81:e50759.
14. Andersen P, Saltin B. Maximal perfusion of skeletal muscle in man. *J Physiol*. 1985;366:233-249.
15. Musch TI, Friedman DB, Pitetti KH, et al. Regional distribution of blood flow of dogs during graded dynamic exercise. *J Appl Physiol*. 1987;1985:2269-2277.
16. Geary GG, Buchholz JN. Selected contribution: effects of aging on cerebrovascular tone and $[Ca^{2+}]_i$. *J Appl Physiol*. 2003;1985:1746-1754.
17. Cipolla MJ, Smith J, Kohlmeyer MM, Godfrey JA. SK_{Ca} and IK_{Ca} Channels, myogenic tone, and vasodilator responses in middle cerebral arteries and parenchymal arterioles: effect of ischemia and reperfusion. *Stroke*. 2009;40:1451-1457.
18. Kelleher RJ, Soiza RL. Evidence of endothelial dysfunction in the development of Alzheimer's disease: is Alzheimer's a vascular disorder? *Am J Cardiovasc Dis*. 2013;3:197-226.
19. Kilkenny C, Browne WJ, Cuthill IC, Emerson M, Altman DG. Improving bioscience research reporting: the ARRIVE guidelines for reporting animal research. *PLoS Biol*. 2010;8:e1000412.
20. McGrath JC, Lilley E. Implementing guidelines on reporting research using animals (ARRIVE etc.): new requirements for publication in BJP. *Br J Pharmacol*. 2015;172:3189-3193.
21. Diaz-Otero JM, Garver H, Fink GD, Jackson WF, Dorrance AM. Aging is associated with changes to the biomechanical properties of the posterior cerebral artery and parenchymal arterioles. *Am J Physiol Heart Circ Physiol*. 2016;310:H365-H375.
22. Kochukov MY, Balasubramanian A, Abramowitz J, Birnbaumer L, Marrelli SP. Activation of endothelial transient receptor potential C3 channel is required for small conductance calcium-activated potassium channel activation and sustained endothelial hyperpolarization and vasodilation of cerebral artery. *J Am Heart Assoc*. 2014;3:e000913.
23. Zhang L, Papadopoulos P, Hamel E. Endothelial TRPV4 channels mediate dilation of cerebral arteries: impairment and recovery in

cerebrovascular pathologies related to Alzheimer's disease. *Br J Pharmacol*. 2013;170:661-670.
24. Behringer EJ, Socha MJ, Polo-Parada L, Segal SS. Electrical conduction along endothelial cell tubes from mouse feed arteries: confounding actions of glycyrrhetinic acid derivatives. *Br J Pharmacol*. 2012;166:774-787.
25. Hayoz S, Pettis J, Bradley V, Segal SS, Jackson WF. Increased amplitude of inward rectifier K^+ currents with advanced age in smooth muscle cells of murine superior epigastric arteries. *Am J Physiol Heart Circ Physiol*. 2017;312:H1203-H1214.
26. Marrelli SP, Johnson TD, Khorovets A, Childres WF, Bryan RM Jr. Altered function of inward rectifier potassium channels in cerebrovascular smooth muscle after ischemia/reperfusion. *Stroke*. 1998;29:1469-1474.
27. Behringer EJ, Segal SS. Tuning electrical conduction along endothelial tubes of resistance arteries through Ca^{2+}-activated K^+ channels. *Circ Res*. 2012;110:1311-1321.
28. Curtis MJ, Bond RA, Spina D, et al. Experimental design and analysis and their reporting: new guidance for publication in BJP. *Br J Pharmacol*. 2015;172:3461-3471.
29. Behringer EJ, Shaw RL, Westcott EB, Socha MJ, Segal SS. Aging impairs electrical conduction along endothelium of resistance arteries through enhanced Ca^{2+}-activated K^+ channel activation. *Arterioscler Thromb Vasc Biol*. 2013;33:1892-1901.
30. Segal SS. Integration and Modulation of Intercellular Signaling Underlying Blood Flow Control. *J Vasc Res*. 2015;52:136-157.
31. Hille B. *Ion Channels of Excitable Membranes*, 3rd edn. Sunderland, Massachusetts, USA: Sinauer; 2001.
32. Chen BR, Kozberg MG, Bouchard MB, Shaik MA, Hillman EM. A critical role for the vascular endothelium in functional neurovascular coupling in the brain. *J Am Heart Assoc*. 2014;3:e000787.
33. Ralevic V. Purines as neurotransmitters and neuromodulators in blood vessels. *Curr Vasc Pharmacol*. 2009;7:3-14.
34. Dietrich HH, Horiuchi T, Xiang C, Hongo K, Falck JR, Dacey RG Jr. Mechanism of ATP-induced local and conducted vasomotor responses in isolated rat cerebral penetrating arterioles. *J Vasc Res*. 2009;46:253-264.
35. Draid M, Shiina T, El-Mahmoudy A, Boudaka A, Shimizu Y, Takewaki T. Neurally released ATP mediates endothelium-dependent hyperpolarization in the circular smooth muscle cells of chicken anterior mesenteric artery. *Br J Pharmacol*. 2005;146:983-989.
36. Welsh DG, Segal SS. Coactivation of resistance vessels and muscle fibers with acetylcholine release from motor nerves. *Am J Physiol*. 1997;273:H156-H163.
37. Joyner MJ, Dietz NM. Sympathetic vasodilation in human muscle (2003). *Acta Physiol Scand*. 2003;177:329-336.
38. Wilson C, Lee MD, McCarron JG. Acetylcholine released by endothelial cells facilitates flow-mediated dilatation. *J Physiol*. 2016;594:7267-7307.
39. Remensnyder JP, Mitchell JH, Sarnoff SJ. Functional sympatholysis during muscular activity. Observations on influence of carotid sinus on oxygen uptake. *Circ Res*. 1962;11:370-380.
40. Faraci FM, Heistad DD. Regulation of the cerebral circulation: role of endothelium and potassium channels. *Physiol Rev*. 1998;78:53-97.
41. Hannah RM, Dunn KM, Bonev AD, Nelson MT. Endothelial SK_{Ca} and IK_{Ca} channels regulate brain parenchymal arteriolar diameter and cortical cerebral blood flow. *J Cereb Blood Flow Metab*. 2011;31:1175-1186.
42. Jackson WF. Endothelial cell ion channel expression and function in arterioles and resistance arteries. In: Levitan I, Dopico AM, eds. *Vascular Ion Channels in Physiology and Disease*. Cham, Switzerland: Springer; 2016:3-36.
43. Sancho M, Samson NC, Hald BO, et al. K_{IR} channels tune electrical communication in cerebral arteries. *J Cereb Blood Flow Metab*. 2017;37:2171-2184.
44. Crane GJ, Walker SD, Dora KA, Garland CJ. Evidence for a differential cellular distribution of inward rectifier K^+ channels in the rat isolated mesenteric artery. *J Vasc Res*. 2003;40:159-168.
45. Longden TA, Nelson MT. Vascular inward rectifier K^+ channels as external K^+ sensors in the control of cerebral blood flow. *Microcirculation*. 2015;22:183-196.
46. Beery AK, Zucker I. Sex bias in neuroscience and biomedical research. *Neurosci Biobehav Rev*. 2011;35:565-572.
47. Scotland RS, Madhani M, Chauhan S, et al. Investigation of vascular responses in endothelial nitric oxide synthase/cyclooxygenase-1 double-knockout mice: key role for endothelium-derived hyperpolarizing factor in the regulation of blood pressure in vivo. *Circulation*. 2005;111:796-803.
48. Sandow SL, Hill CE. Incidence of myoendothelial gap junctions in the proximal and distal mesenteric arteries of the rat is suggestive of a role in endothelium-derived hyperpolarizing factor-mediated responses. *Circ Res*. 2000;86:341-346.
49. Bagher P, Beleznai T, Kansui Y, Mitchell R, Garland CJ, Dora KA. Low intravascular pressure activates endothelial cell TRPV4 channels, local Ca^{2+} events, and IK_{Ca} channels, reducing arteriolar tone. *Proc Natl Acad Sci USA*. 2012;109:18174-18179.
50. Sandow SL, Neylon CB, Chen MX, Garland CJ. Spatial separation of endothelial small- and intermediate-conductance calcium-activated potassium channels K_{Ca} and connexins: possible relationship to vasodilator function? *J Anat*. 2006;209:689-698.
51. Sonkusare SK, Dalsgaard T, Bonev AD, et al. AKAP150-dependent cooperative TRPV4 channel gating is central to endothelium-dependent vasodilation and is disrupted in hypertension. *Sci Signal*. 2014;7:ra66.
52. Tran CH, Taylor MS, Plane F, et al. Endothelial Ca^{2+} wavelets and the induction of myoendothelial feedback. *Am J Physiol Cell Physiol*. 2012;302:C1226-C1242.
53. Tran CH, Gordon GR. Astrocyte and microvascular imaging in awake animals using two-photon microscopy. *Microcirculation*. 2015;22:219-227.
54. Socha MJ, Behringer EJ, Segal SS. Calcium and electrical signalling along endothelium of the resistance vasculature. *Basic Clin Pharmacol Toxicol*. 2012;110:80-86.
55. Muller-Delp JM, Gurovich AN, Christou DD, Leeuwenburgh C. Redox balance in the aging microcirculation: new friends, new foes, and new clinical directions. *Microcirculation*. 2012;19:19-28.
56. McCarron JG, Halpern W. Impaired potassium-induced dilation in hypertensive rat cerebral arteries does not reflect altered Na+, K + -ATPase dilation. *Circ Res*. 1990;67:1035-1039.
57. Crossland RF, Durgan DJ, Lloyd EE, et al. A new rodent model for obstructive sleep apnea: effects on ATP-mediated dilations in cerebral arteries. *Am J Physiol Regul Integr Comp Physiol*. 2013;305:R334-R342.
58. Tajbakhsh N, Sokoya EM. Compromised endothelium-dependent hyperpolarization- mediated dilations can be rescued by NS309 in obese Zucker rats. *Microcirculation*. 2014;21:747-753.

How to cite this article: Hakim MA, Buchholz JN, Behringer EJ. Electrical dynamics of isolated cerebral and skeletal muscle endothelial tubes: Differential roles of G-protein-coupled receptors and K^+ channels. *Pharmacol Res Perspect*. 2018;e00391. https://doi.org/10.1002/prp2.391